

A common stochastic accumulator with effector-dependent noise can explain eye-hand coordination

Atul Gopal,¹ Pooja Viswanathan,¹ and Aditya Murthy²

¹National Brain Research Centre, Manesar, Haryana, India; and ²Centre for Neuroscience, Indian Institute of Science, Bangalore, Karnataka, India

Submitted 10 October 2014; accepted in final form 6 January 2015

Gopal A, Viswanathan P, Murthy A. A common stochastic accumulator with effector-dependent noise can explain eye-hand coordination. *J Neurophysiol* 113: 2033–2048, 2015. First published January 7, 2015; doi:10.1152/jn.00802.2014.—The computational architecture that enables the flexible coupling between otherwise independent eye and hand effector systems is not understood. By using a drift diffusion framework, in which variability of the reaction time (RT) distribution scales with mean RT, we tested the ability of a common stochastic accumulator to explain eye-hand coordination. Using a combination of behavior, computational modeling and electromyography, we show how a single stochastic accumulator to threshold, followed by noisy effector-dependent delays, explains eye-hand RT distributions and their correlation, while an alternate independent, interactive eye and hand accumulator model does not. Interestingly, the common accumulator model did not explain the RT distributions of the same subjects when they made eye and hand movements in isolation. Taken together, these data suggest that a dedicated circuit underlies coordinated eye-hand planning.

drift diffusion; reaction time; variability; electromyography; motor preparation; eye-hand coordination

ALTHOUGH STOCHASTIC ACCUMULATION of information has provided a general framework to explain behavior in a multitude of reaction time (RT) tasks for a variety of effectors in isolation (Carpenter and Williams 1995; Ratcliff 1978; Ratcliff and Van Dongen 2011; Reddi et al. 2003), its ability to explain the RTs of combined eye-hand movements has surprisingly received scant attention. In a recent study, Dean et al. (2011) examined how cross coupling between otherwise independent eye and hand accumulators can explain correlations between the RTs of eye and hand when engaged in a coordinated motor behavior. In contrast, the common motor command model (Biguer et al. 1982; Bizzi et al. 1971; Bock 1987), which hypothesizes that eye and hand movements are planned and initiated by a common signal, has been an influential framework that has motivated numerous experiments to understand the mechanisms involved in eye-hand coordination (Bekkering et al. 1994; Fisk and Goodale 1985; Mather and Fisk 1985; Sailer et al. 2000). In concurrence with the common command model, numerous studies have shown the presence of high correlations between eye and hand RTs in a variety of tasks involving eye-hand movements in humans as well as nonhuman primates (Herman et al. 1981; Rogal et al. 1985). This evidence notwithstanding, a number of studies (Gielen et al. 1984; Mather and Fisk 1985) have shown modest eye-hand RT correlations. More importantly, the common command model has not been

subject to quantitative assessment, and hence the nature and extent of effector-independent (common) and effector-dependent representations underlying eye-hand coordination remain unspecified. Here, we attempt a critical step toward this direction by testing and predicting the ability of a single common accumulator model to explain eye-hand RTs and their correlations.

MATERIALS AND METHODS

We recorded 24 normal subjects (23 right handed, 1 left handed, 20 men and 4 women), between 25 and 28 yr of age with normal or corrected-to-normal vision in 3 different tasks involving visually-guided pointing. All subjects gave their informed consent in accordance with the institutional human ethics committee, which reviewed and approved the experimental protocol. Subjects were monetarily rewarded for their participation in the study.

For the initial 8 subjects (*experiment 1*) we used a redirect task, which is a modified version of a double-step paradigm, with an implicit countermanding signal incorporated in it (Ramakrishnan et al. 2010; Ray et al. 2004). Two types of trials were randomly interleaved. No-step trials (60%) began when a white fixation target appeared at the center of the screen and subjects were instructed to fixate and point with their index finger to it. When subjects maintained fixation and held the pointing finger steady, for a fixation period of 300 ± 100 ms (accurate to the screen refresh rate of 60 Hz), a peripheral green target appeared, either to the right or left of the fixation target, at an eccentricity of 12° . Subjects were instructed to make a saccade and point, as quickly and accurately as possible, to the green target (Fig. 1A).

During the remaining 40% of the trials, known as step trials, the green target was followed by a yellow target that appeared in the opposite hemifield (180°) with the same eccentricity (12°). On these trials, the yellow target served as a redirect cue, instructing the subjects to inhibit their intended response (pointing and saccade) to the initial target and to execute a new response to the final target, instead. Target step delay (TSD), the time between the appearances of the final target relative to that of the initial target, was varied randomly from trial to trial. Step trials, however, are not the subject of the present paper.

Trial Conditions

Subjects were recorded on the redirect task with three different conditions during separate sessions.

Eye-alone. During the eye-alone condition subjects were instructed to perform the task with saccades, while their pointing finger was positioned at fixation. A trial was aborted when the pointing finger left the fixation box during the trial. Six hundred trials were recorded per subject under the eye-alone condition with six TSDs ranging from 34–284 ms, accurate to the nearest integer refresh rate, in steps of ~ 50 ms.

Hand-alone. During the hand-alone condition subjects were instructed to perform the task with their hand while they maintained

Address for reprint requests and other correspondence: A. Murthy, Centre for Neuroscience, Indian Institute of Science, Bangalore 560012, Karnataka, India (e-mail: aditya@cns.iisc.ernet.in).

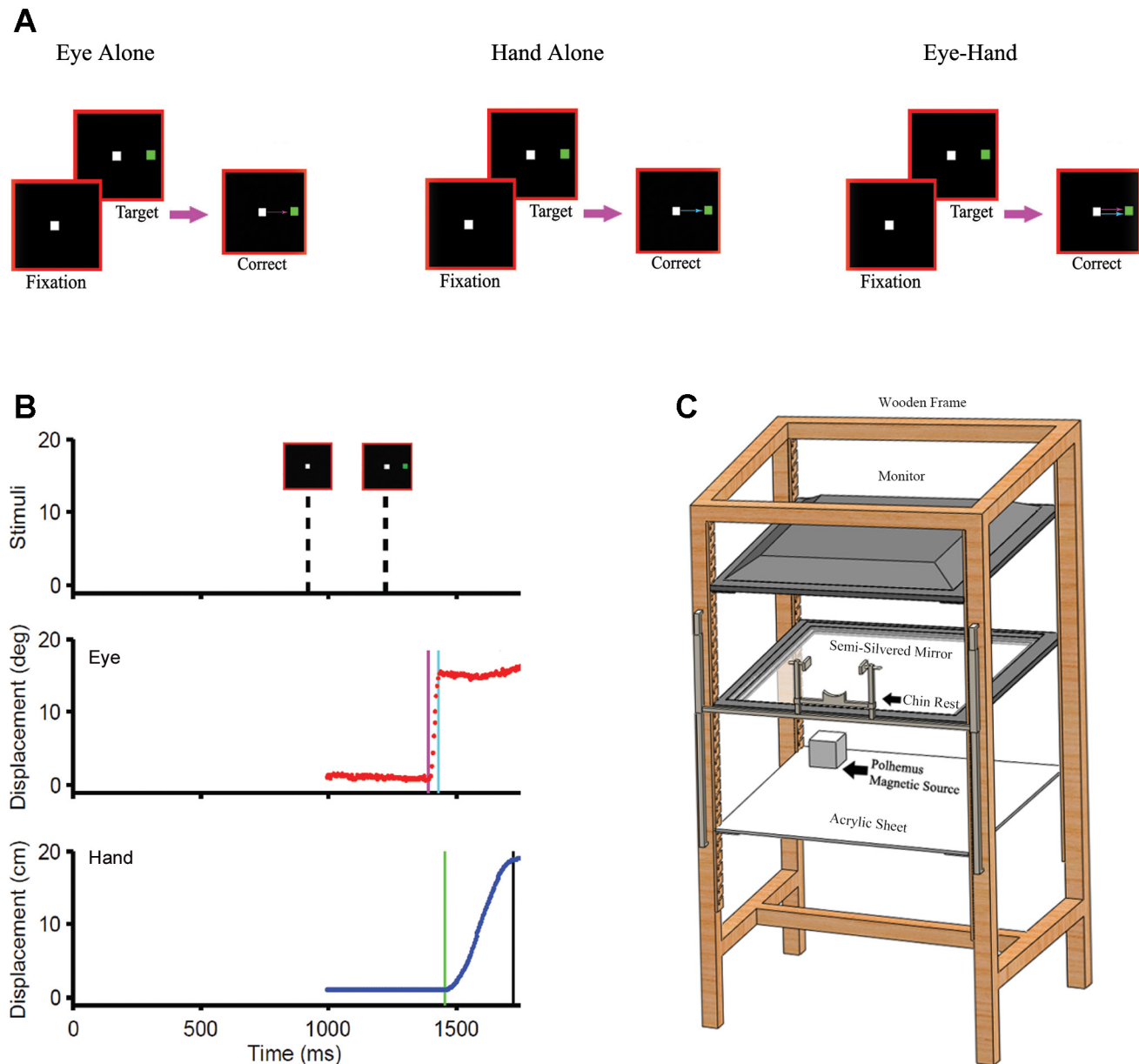


Fig. 1. The task. *A*: in the eye-alone, hand-alone and eye-hand conditions, subjects were instructed to make a saccade, pointing movement, or both, respectively, to targets that could appear 12° on either side of the fixation box. *B*: temporal sequence of events in a typical no-step trial. The *top* panel shows the sequence of stimuli the subject viewed. The *middle* and *bottom* panels show successive eye and hand positions, respectively. The start and the end of the saccade are marked by the pink and the cyan lines, respectively, and that of the hand movement, by the green and the black lines, respectively. *C*: schematic of the experimental setup.

their gaze at fixation. A trial was aborted when the eye left the fixation box along with the hand during the trial. Seven hundred trials were recorded per subject under the hand-alone condition with seven TSDs ranging from 134–734 ms, accurate to the nearest integer refresh rate, in steps of ~ 100 ms.

Eye-hand. During the eye-hand condition subjects were instructed to perform the redirect task with both their eyes and the hands together. In step trials only those trials in which both the eye and the pointing finger satisfied the redirect condition were considered successful. One thousand trials were recorded per subject under the eye-hand condition with 10 TSDs. The values of TSDs used in the eye-hand condition were a combination of those used in the eye-alone and hand-alone conditions.

To ensure that the presence of step trials had no bearing on the no-step analyses, we recorded an additional 12 subjects in an

eye-hand task with only no-step trials (*experiment 2*). We also recorded the EMG from the shoulder muscle (anterior deltoid) while these subjects performed the no-step task. To assess within-subject variability, we tested 4 subjects in a second session and found their EMG onsets to be significantly different from the first session. Hence we treated the second session as an independent observation to obtain a total of 16 sessions with eye-hand and concurrent EMG data. In addition, four separate subjects were recorded while they performed no-step trials in the hand-alone condition along with simultaneous recording of their EMG (*experiment 3*).

Trials were scored as successful if subjects fixated the target within $\pm 5^\circ$. This was determined online by means of an electronic window centered on the target. Auditory feedback was given to the subjects on all successful trials.

Setup for Data Acquisition

The experiment was under the control of TEMPO/VDOSYNC software (Reflective Computing), which displayed visual stimuli and recorded data at a temporal resolution of 1 ms. Eye movements were monitored by a noninvasive video-based pupil tracker (ISCAN) at a sampling frequency of 240 Hz, which interfaced with TEMPO in real time with a delay of 8 ms. Hand movements were tracked by an electromagnetic tracker (LIBERTY, Polhemus) that read the movement of a sensor in a magnetic field created by a source at a sampling frequency of 240 Hz. The hand tracker was also interfaced with TEMPO in real time with a delay of $8 \text{ ms} \pm 1 \text{ ms}$. EMG activity from the anterior deltoid muscle of the performing hand was recorded in differential mode using 10-mm gold cup electrodes (Care Fusion). The recording electrode was placed on the belly of the anterior deltoid muscle, the reference electrode at the point of insertion of the same muscle at the shoulder, and the ground electrode was placed on the elbow away from the recording site. Signals were band passed between 10 and 250 Hz, notch filtered at 50 Hz, amplified (Blackrock Microsystems), and digitized in TEMPO with a temporal resolution of 1 ms.

Stimuli were presented on a CRT monitor (Sony SGI, 21-in., 60-Hz refresh rate) or an LCD monitor (Dell, 20-in., 60-Hz refresh rate). A plane mirror (25% transmission, 75% reflectance) was placed below the monitor at an angle, to reflect the monitor display. An acrylic sheet was kept in the same plane as that of the virtual image of the monitor, on which subjects performed the pointing movement. The sheet constrained the movement of the hand in one plane. This virtual reality setup (Fig. 1C; adapted from the laboratory of Dr. Neggers, Univ. Of Utrecht) was preferred to minimize the distortion caused by the electrostatic and electromagnetic fields of the CRT monitor on the electromagnetic tracker and facilitate eye tracking simultaneously.

Recording Procedure

Subjects were comfortably seated in a position to foveate and point at the virtual image of the monitor formed by the mirror. A sensor was strapped with Velcro on the pointing finger to track hand position, along with a battery-powered LED for visual feedback. Head movements were minimized by clamping the chin, forehead and temple. Subjects were recorded on different trial conditions, on separate days, in separate blocks. At the beginning of each session subjects were given written and verbal instructions, followed by some practice trials (~50) before the data were collected. On average, subjects performed about 500 trials per session, with breaks after every 250 trials. A typical session lasted about 1 h, and a subject had to perform five to eight sessions to complete the dataset. Calibrations were performed by having subjects point and fixate at the two target positions.

Analysis

All analyses and statistical testing were done offline using MATLAB (Mathworks). Blinks were detected using velocity thresholds ($>800^\circ/\text{s}$) and verified manually. The trials with blink perturbed saccades were removed from further analysis. Custom programs were written in MATLAB to detect saccadic and hand movements from the raw data containing instantaneous X and Y positions of both effectors. A velocity threshold of $30^\circ/\text{s}$ was used to mark the beginning and end of a saccade, while a threshold 10 cm/s was used to mark the start and end of a pointing movement. To detect the onset of EMG activity, the raw EMG signal was rectified and smoothed using a boxcar filter with a temporal window of 20 ms duration. The time at which the poststimulus EMG activity increased by more than 5 standard deviations from the baseline activity was considered the EMG onset. The digitized eye and hand traces along with the detected onsets and offsets in a typical trial are shown in Fig. 1B. Although RT distributions of individual subjects are skewed, the distribution of mean RTs

across the population are normal, as assessed by a Lilliefors test. Thus, means and SDs were typically reported and used for statistical analyses performed in MATLAB. Unless indicated otherwise, statistical significance was tested using either one- or two-tailed t -tests, where appropriate.

Modeling RT Distributions

We modeled the behavior of subjects in no-step trials using a diffusion type accumulator model of movement initiation (Ratcliff and Van Dongen 2011; Usher and McClelland 2001). The model comprises a GO process that instantiates the accumulation of activity to threshold responsible for movement initiation. The GO process accumulates noisy sensory evidence after a visual delay of 60 ms. This accumulation is thought to represent preparatory activity build-up toward a threshold that initiates movement (Schall and Hanes 1998). The level of accumulation at each time step is governed by a stochastic equation given below:

$$a_{GO}(t) = a_{GO}(t-1) + \mu_{GO} + \xi_{GO} \quad (1)$$

where, a_{GO} represents GO unit activation at time t ; the mean GO or drift rate is given by μ_{GO} , which represents the mean strength of the sensory signal; ξ is the Gaussian noise term with mean of 0 and standard deviation of σ , which represents noise in the sensory signal. The rate of accumulation was modeled as ideal (without leak) and stochastic across each time step of 1 ms. Such a drift diffusion process produces a stochastic trajectory of preparatory activity that reaches threshold at different time points for different trials, resulting in a distribution of RTs. Using numerical simulations, we verified that the mean and the SD of the resultant RT distributions were monotonically related (Wagenmakers et al. 2005).

To estimate these parameters (μ_{GO} and σ_{GO}), we used Monte Carlo simulations. We simulated 2,000 no-step trials in each iteration by randomly selecting values for μ_{GO} and σ_{GO} , separately for each subject. We used the Kolmogorov-Smirnov (KS) statistic to compare the simulated and observed no-step cumulative RT distributions. Convergence was decided based on parameter values that minimized the KS statistic between the simulated and observed data (Reddi and Carpenter 2000). Minimization was carried out using MATLAB's `fmincon`, a nonlinear minimization function, which ran 1,000 such iterations. Convergence occurred on a typical run within 20 iterations. We repeated this procedure 100 times, with different sets of random initial starting conditions that tiled the parameter space typically observed for generating RT distributions before choosing the best set of parameters. The set of parameters that resulted in the smallest value of the KS statistic was chosen as the optimal solution. The whole procedure was repeated to ensure the reliability of the estimated parameters. The μ and σ parameters estimated separately for the eye and hand effectors, based on their respective RT distributions, constituted the free parameters for all the models.

To test whether our Monte Carlo simulations provided us with the best estimates of the underlying distribution, we performed different benchmarking tests. An RT distribution with 10,000 trials was simulated with known parameters of μ_{GO} and σ_{GO} . We verified that the Monte Carlo method converged to the same values, given only the RT distribution. We also tested a brute force method in which the entire parameter space was assessed and found convergence to the same value reported by the Monte Carlo simulation. Although local minima were also detected, the error between the predicted and the observed RT associated with these parameters in the local minima was higher. Thus the criterion of choosing the parameters associated with the least error values as the best fit parameters ensured that simulations converged to the best solution.

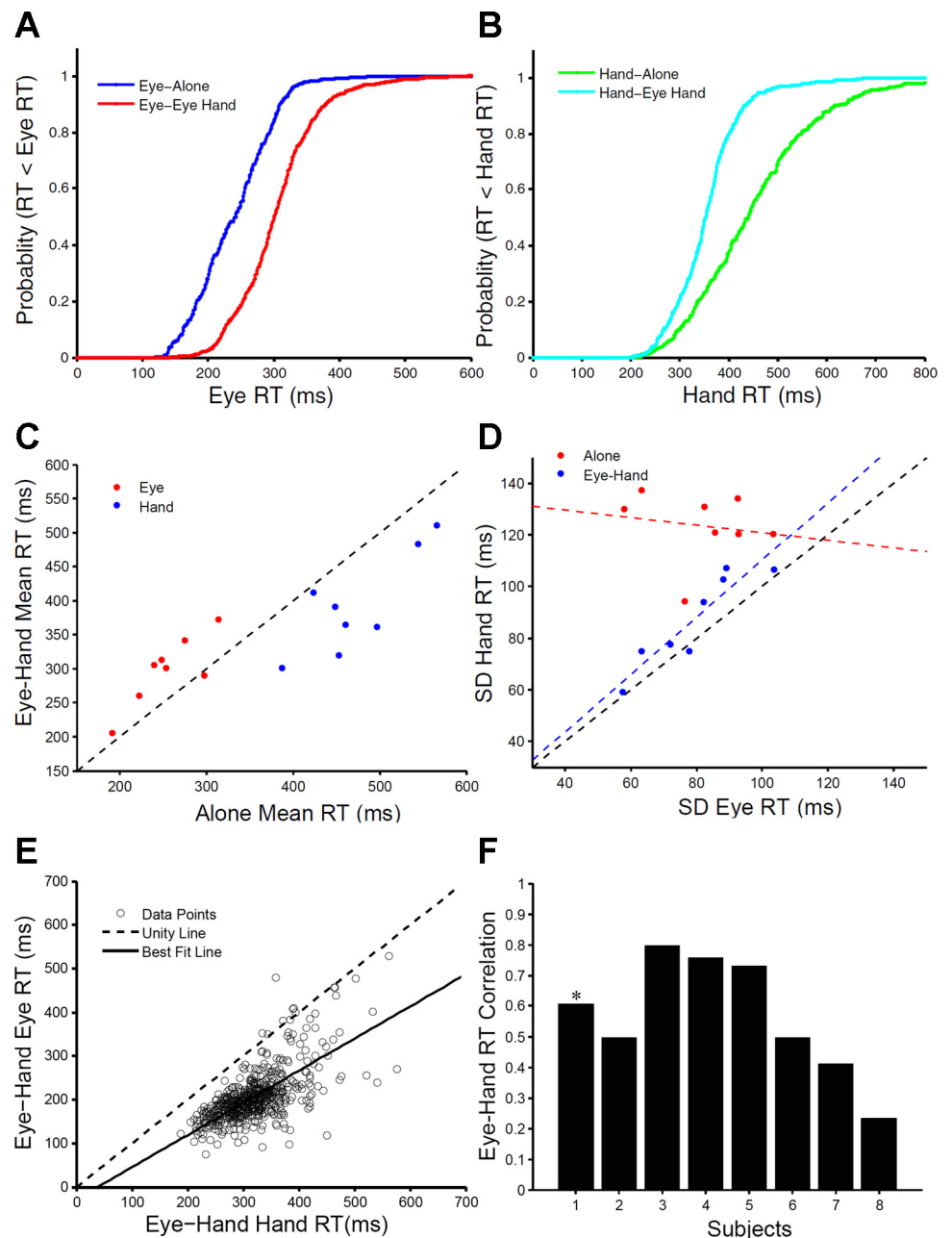
The Common Command Model

To test the common command hypothesis, we implemented the model in MATLAB and simulated 2,000 trials. We assumed that a common accumulator, representing both eye and hand movement preparation, could be modeled using the eye RT data as a proxy of the central command. The hand RT distribution was simulated in a similar fashion as described above, using the best fit eye parameters (μ_{GO} and σ_{GO}), after incorporating either a delay (delay model) or higher threshold (threshold model), randomly chosen from a range of values. We used the KS statistic to compare the simulated and observed no-step hand cumulative RT distributions. The KS statistic was minimized in the parameter space using a nonlinear minimization procedure (fmincon) in MATLAB. We repeated this procedure 100 times, with different sets of initial parameter values, before choosing the best value for the delay and threshold parameter. The parameters estimated for either the delay or the threshold were also free parameters in the common command model.

RESULTS

To determine whether the programming of a saccadic eye movement was influenced by the concurrent programming of a hand movement and vice versa, we analyzed RTs when eight subjects (*experiment 1*) performed eye-alone and hand-alone movements separately vs. when they performed them together (eye-hand) (Fig. 1A). Figure 2, A and B, shows the RT of a typical subject. A similar trend was observed across all subjects (Fig. 2C). Across the population, compared with the eye-alone condition (255 ± 40 ms), mean saccade RT in the eye-hand condition (eye_{eh} RT = 299 ± 50 ms) increased by 44 ms on average ($n = 7/8$ subjects, max = 67 ms, min = 13 ms, $P = 0.001$). In contrast, the mean RT (472 ± 60 ms) for hand-alone compared with the mean hand RT in the eye-hand condition (hand_{eh} RT = 392 ± 74 ms) decreased by 80 ms on average for eye-hand movements (Fig. 2B; $n = 8/8$ subjects,

Fig. 2. Behavior in eye-hand vs. eye-alone and hand-alone conditions. **A**: saccade reaction time (RT) in the eye-hand condition (red) is delayed compared with the eye-alone condition (blue). **B**: hand RT in the eye-hand condition (cyan) is faster than in the hand-alone condition (green). **C**: scatter plot of the mean saccade and hand RT between the alone vs. the eye-hand condition for the population. The unity line is shown for reference. Mean saccade RTs (red) above the unity line suggest a slower saccade RT in the eye-hand condition, while mean hand RTs (blue) below the unity line suggest faster RT for the hand in the eye-hand condition. **D**: scatter plot of the saccade and hand RT standard deviations (SDs) across subjects. The data points in the coordinated condition (blue) follow the unity line (black dashed line), suggesting that variability in the saccade and hand RTs is comparable. The SDs of the hand-alone RTs are greater than the SDs of the eye-alone RTs as the data points (red) lie above the unity line. The best fit lines for the coordinated (blue) and alone (red) conditions are shown as dashed lines. **E**: scatter plot of individual saccade and hand RTs in the eye-hand condition plotted for a typical subject shows a strong correlation. The best fit line is shown as the black solid line and the unity line as the black dashed line. **F**: Pearson's correlation coefficients calculated between the saccade and hand RT in the eye-hand condition across subjects. The asterisk denotes the data from the subject shown in **E**.



max = 135 ms, min = 11 ms, $P = 0.001$). In addition, mean saccade and hand RT standard deviations (SDs) were 82 ± 16 ms and 123 ± 13 ms in the eye-alone and hand-alone conditions, respectively, and were significantly different (Fig. 2D; $P < 0.001$). In contrast, mean saccade and hand RT SDs were 79 ± 15 ms and 87 ± 16 ms, respectively, in the eye-hand condition, and were not significantly different (Fig. 2D; $P = 0.3515$), even though their respective means were significantly different ($P = 0.001$).

We also tested whether saccade and hand RTs were correlated. The scatter plot of RT during the eye-hand condition, for a representative subject is depicted in Fig. 2E. The Pearson's correlation coefficient for this subject was 0.60 ($P < 0.001$), indicating a strong temporal correlation between the two effectors. A similar trend was observed across the population (mean = 0.56 ± 0.19 , max = 0.79, min = 0.23, $P < 0.05$ for all subjects; Fig. 2F).

The Common Command Model

Many studies have shown that SDs of typical RT distributions scale with mean RT (Luce 1986; Wagenmakers and Brown 2007). Such an empirical relation is naturally explained by the drift diffusion framework since an increase in mean RT is accounted for by a longer duration of stochastic accumulation, producing greater RT variability (Wagenmakers et al. 2005). In the context of eye-hand coordination, such a drift diffusion framework envisages that, since the mean hand RT is greater than mean eye RT, the SDs of their respective RT distributions should also scale accordingly. We used this relationship to test whether, and the extent to which a common command, as opposed to independent eye and hand accumulators, underlies eye-hand coordination. We found that, even though the mean hand RT distributions were significantly greater than the mean eye RT distributions in the eye-hand condition across subjects by 94 ± 40 ms ($P = 0.001$), mean SDs of the hand RT distributions did not scale with the larger mean hand RTs. Interestingly, the difference in mean saccade and hand SDs across subjects was only 7 ± 7 ms and were not statistically significant ($P = 0.3515$). The similarity of the SD of the eye and hand RT distributions suggests that the planning of eye-hand movements is amenable to simulation by a single drift diffusion process. It also implies that the additional time taken by the hand may reflect a delay intrinsic to the hand effector system, which, not being part of the accumulator process, does not add to the observed variability of the hand RT in the eye-hand condition.

We verified the common command assumption by fitting the eye and hand RT distributions with a single accumulator based on the eye RT distribution. Differences in the mean eye and hand RTs within the framework of a common command model can, in principle, be accounted by two architectures shown in Fig. 3, A and B: a delay incorporated into the planning of the hand movement (delay model) or a differential threshold for the eye and hand (threshold model). In the context of drift diffusion, both of these models have different predictions. In the threshold model, if the greater hand RT is due to a higher threshold for the hand accumulator relative to the eye accumulator, then hand RT variance is expected to be likewise greater than the eye RT variance, as a consequence of stochastic accumulation for a longer duration. Therefore, the slope of the

best fit line between the predicted and observed RT variances across subjects should produce a slope greater than unity. In contrast, the delay model does not contain any additional stochastic accumulation for the hand RT. Therefore, the best linear fit of the comparison of predicted with observed RT variance across subjects should produce a slope closer to the unity line. Figure 3, C and D, shows the best fits of hand RT distributions for each model in a typical subject. Although both models fit the mean hand RT distributions across subjects (Fig. 3E), the slope of the best fit linear regression for the hand RT variance was closer to unity in the delay model (1.15) compared with the threshold model (1.73) (Fig. 3F; $P = 0.06$). Hence, the delay model better explained the data than the threshold model.

Testing the Common Command Model

Since the previous data set was derived from a redirect task in which the subjects were also asked to cancel their planned responses in case the second target appeared (see MATERIALS AND METHODS), we also measured coordinated eye-hand RTs in a separate experiments (*experiment 2*) comprising 16 different sessions (12 subjects; 4 subjects with 2 sessions), to ensure that the presence of step trials did not confound the basic result. In congruence with the results presented in Fig. 2, we found that the mean saccade and hand RT distributions were significantly different from each other ($P < 0.001$), while the SDs of the same distributions were comparable ($P = 0.77$) (see Fig. 5A).

In *experiment 2*, subjects made pointing movements while their EMG activity from the anterior deltoid muscle was obtained. The EMG measurement allowed us to test the delay model. Because the range of delays predicted by the model was between 40 and 150 ms and fell within the reported range of the time interval between the onset of EMG and the start of the hand movement (Gribble et al. 2002; Karst and Hasan 1991), we hypothesized that the neural correlate of the delay was the time interval between the onset of EMG and the start of the hand movement, also sometimes referred to as the electromechanical delay (see Fig. 4). In congruence with previous work, the mean delay measured from the EMG was 160 ± 23 ms. The predictions of the common command model, however, underestimated the observed delay (mean predicted delay = 118 ± 41 ms; $P < 0.001$). This underestimation by the model is expected because we used the saccade RT distribution to constrain the parameters of the common accumulator, while EMG onsets may indicate the termination of the common central component of the movement preparation which can happen prior to saccade onset.

To test whether EMG onsets demarcate the termination of the common central component of the movement planning, we tested the trial-by-trial relationship between EMG onsets and hand onsets as well as saccade onsets (Fig. 5B). Since EMG onsets precede the hand onsets, we found a strong significant temporal correlation (0.79 ± 0.07). Interestingly, we also found that saccade onsets were also strongly correlated (0.65 ± 0.17) with EMG onsets. In addition, the partial correlation was also significant ($r = 0.50 \pm 0.2$) across 16 sessions, suggesting a relation between saccade onset and EMG onset without the influence of the concomitant hand movement. To further test for the signature of a common command, we compared the SDs of eye and hand RTs with the SDs of the EMG latency

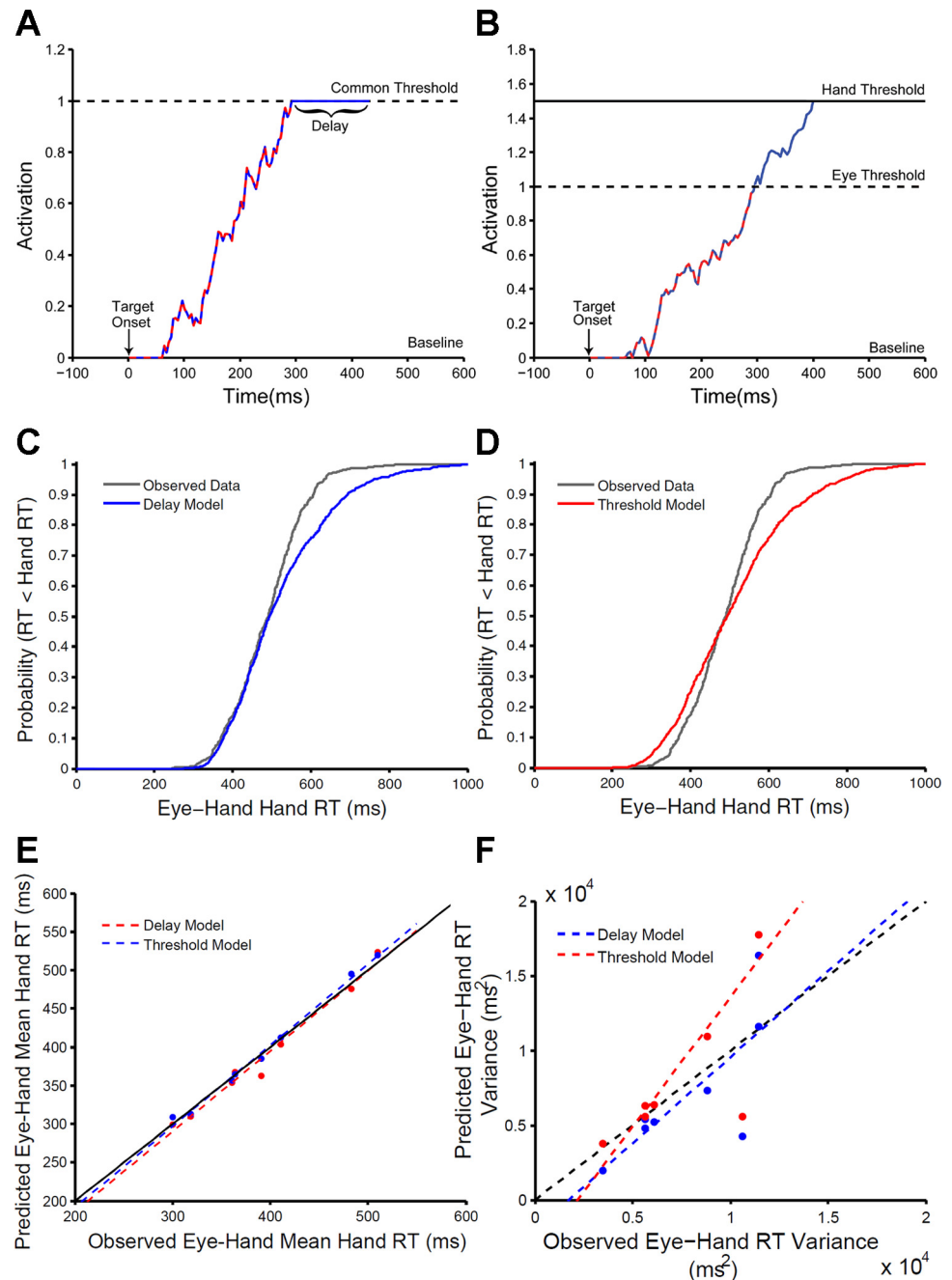


Fig. 3. Modeling eye-hand behavior using a common command. *A* and *B*: schematic representing the common command model. The dashed red-blue trace represents a common signal for initiating eye and hand effectors. Movements are initiated when the common command reaches threshold. The common command model can be implemented either with a temporal delay (*A*) or a differential threshold (*B*) to ensure the proper temporal order of saccade and hand execution. *C* and *D*: cumulative hand RT distribution (gray) in the eye-hand condition compared with the predicted RT distribution by the delay scheme (blue in *C*) and the threshold scheme (red in *D*). *E*: scatter plot of the observed and predicted mean hand RT by the delay scheme (blue) and the threshold scheme (red) and their respective best fits. Mean RT can be explained by both schemes. *F*: scatter plot of the observed and predicted RT variance by the delay (blue) and threshold schemes (red) and their respective best fits. The delay model is a better predictor of the hand RT variance since it is closer to the line of unity slope (dashed black).

distribution (from target onset). As predicted, we observed that the SD of the EMG latency and hand RT distributions were comparable ($P = 0.44$) and highly correlated ($r = 0.91$, $P < 0.001$). More interestingly, we also found strong correlations between the SD of the EMG latency and saccade RT distributions ($r = 0.91$, $P < 0.001$), and the SD of these two distributions were also comparable ($P = 0.29$) (Fig. 5*C*). Taken together, these data suggest that EMG onsets can be considered a proxy measure of the central common command for eye and hand movement plans.

Although EMG onsets were correlated with saccade onsets, EMG onset typically occurred prior to saccade onset (Fig. 4), even though the hand movement occurred after saccade onset. We therefore hypothesized that the observed latency difference may be due to the delay between the threshold of the common

command and the saccade onset. We therefore plotted the distribution of delays (Fig. 4*B*) between the EMG onset and saccade onset and observed that the hand EMG onset occurred 39 ± 25 ms before the saccade for the representative subject and across all 16 sessions (Fig. 5*D*, mean = 54 ms, max = 102 ms, min = 18 ms). We, therefore, used the time difference between EMG onset and saccade onset as an estimate of the oculomotor delay, as it agrees well with the reported values in the literature (Robinson 1972; Schiller and Stryker 1972; Straschill and Rieger 1973). After incorporating the saccade delay into the common command model, the predicted and the observed hand delays became comparable ($P = 0.92$). Moreover, we also found a strong correlation (Fig. 5*E*) between the hand delay measured using EMG and the hand delays predicted by the common command model ($r = 0.51$, P value = 0.04, $n = 16$).

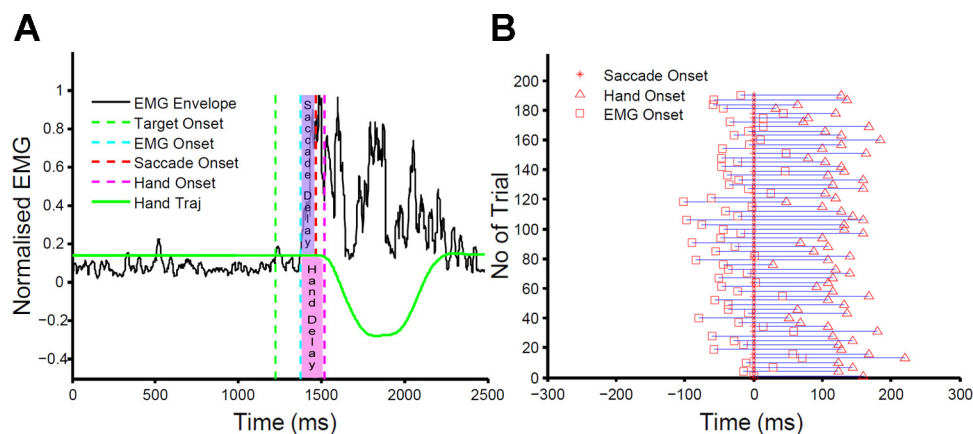


Fig. 4. Characterization of the EMG signal with respect to hand and saccadic movement onset. A: root mean square of the normalized EMG signal (black) recorded from the anterior deltoid muscle. EMG onset (cyan), saccade onset (red) and hand movement onset (magenta) are also shown for reference. B: EMG and hand onsets aligned to saccade onset showing EMG onset occurred prior to saccade onset.

In addition, we also observed, on average, a smaller fraction of trials (37%) across the population in which the EMG onsets occurred after the saccade, resulting in a counterintuitive negative saccade delay. In principle, these trials may reflect instances when the common command model cannot explain the data. To test this, we grouped the trials into two sets: trials in which EMG onset occurs prior to saccade onset, and trials in which EMG onset occurs after saccade onset. We compared the SDs of the eye and hand RT distributions in each group separately. We hypothesized that, if trials with EMG onset after saccade onset reflect violations of the common command model, then the SDs of eye and hand RTs would scale linearly, since their means were significantly different. Contrary to this hypothesis, we found that the SDs of eye and hand RTs were comparable for trials in which EMG onset occurred after saccade onset ($P = 0.23$), similar to trials in which EMG onset occurred before saccade onset ($P = 0.56$). We also found a robust eye and hand RT correlation for trials in which EMG onset was detected after saccade (0.78 ± 0.15), which was comparable ($P = 0.16$) to the RT correlation in trials in which EMG onset was detected before saccade (0.67 ± 0.24). These results suggest that trials with negative saccade delays may not reflect violations of the common command model. We also tested whether noise in the signal delayed the detection of EMG onset, resulting in trials with negative saccade delays. Consistent with this idea, we found the trials with EMG onset detected after saccade onset to be typically associated with large baseline noise compared with the trials in which EMG onset was detected earlier. To quantify this effect, the SD of the averaged baseline RMS signal for trials in which the EMG onset either preceded or followed saccade onset was computed. We found that the SD of the average baseline activity in the trials in which the EMG onset was detected after saccade onset was significantly greater (64 ± 41 arbitrary units, $P = 0.04$) than trials in which EMG onset was detected before saccade onset (38 ± 25 arbitrary units).

The common command model further assumes that the hand delays are pure temporal delays during which no accumulation happens. We hypothesized that if the estimated hand delay from EMG is a pure temporal delay, then its variability is expected to be independent of the mean estimated delay (Fig. 5F). To test this, the Pearson correlation coefficient was calculated between the means and SDs of the hand delay calculated from the EMG across all the sessions and was found to be negligible and nonsignificant ($r = 0.25$, $P = 0.36$, $n = 16$). In

contrast, the variability and mean saccade delay were highly correlated ($r = 0.8$, P value < 0.001 , $n = 16$).

Although a central common command model is expected to generate perfect eye-hand RT correlations, presumably the trial-to-trial variability in effector-specific delays is a prime driver of the observed eye-hand RT correlations. To test this, we computed the SD of the predicted and observed delay distributions, operationally defined here as hand motor noise. A comparison between the predicted and observed hand motor noise showed that they were well correlated (Fig. 6A, $r = 0.84$, $P < 0.001$, $n = 16$). Most importantly, the hand motor noise calculated from the EMG and the correlation between the RT of the eye and hand were negatively correlated (Fig. 6B, $r = -0.81$, $P < 0.001$, $n = 16$). Likewise, we also observed a similar inverse relation between the predicted hand motor noise and eye-hand RT correlations ($r = -0.72$, $P < 0.001$, $n = 16$, Fig. 6C). These data strongly implicate motor noise as a strong determinant in de-correlating the temporally structured eye-hand signal, emanating as a consequence of the common motor command. In addition, the Pearson's correlation coefficient between eye and hand delays across trials for each session was high (mean = 0.43 ± 0.13 , max = 0.63 , min = 0.15 , $P < 0.001$ for all sessions). Interestingly, we observed a trend that the delay correlations shared a linear relationship ($r = 0.46$, $P = 0.09$, $n = 14$ sessions) with the observed eye-hand RT correlations, suggesting that the RT correlations may reflect covariation in motor noise.

The above results were obtained by treating each session as an independent measure, since we observed sufficient variability across each repeat session ($n = 4$; 12 subjects, 16 sessions). Therefore, we also tested whether the basic results held up by considering each subject, not each session, as an independent measure. As shown earlier, the mean SDs of eye and hand RT distributions were not statistically different from each other ($P = 0.40$). The predicted and observed delays ($r = 0.62$, $P = 0.04$, $n = 11$) were correlated. (The mean hand delay estimated for 2 sessions of the remaining one subject was 38 ms apart. Since pooling these sessions together gave an unreliable estimate of the mean, they were not included in this analysis.) Motor noise was also correlated ($r = 0.562$, $P = 0.057$, $n = 12$). RT correlations between eye and hand RT distributions and those predicted by the common command model were also correlated ($r = 0.92$, $P < 0.001$, $n = 12$).

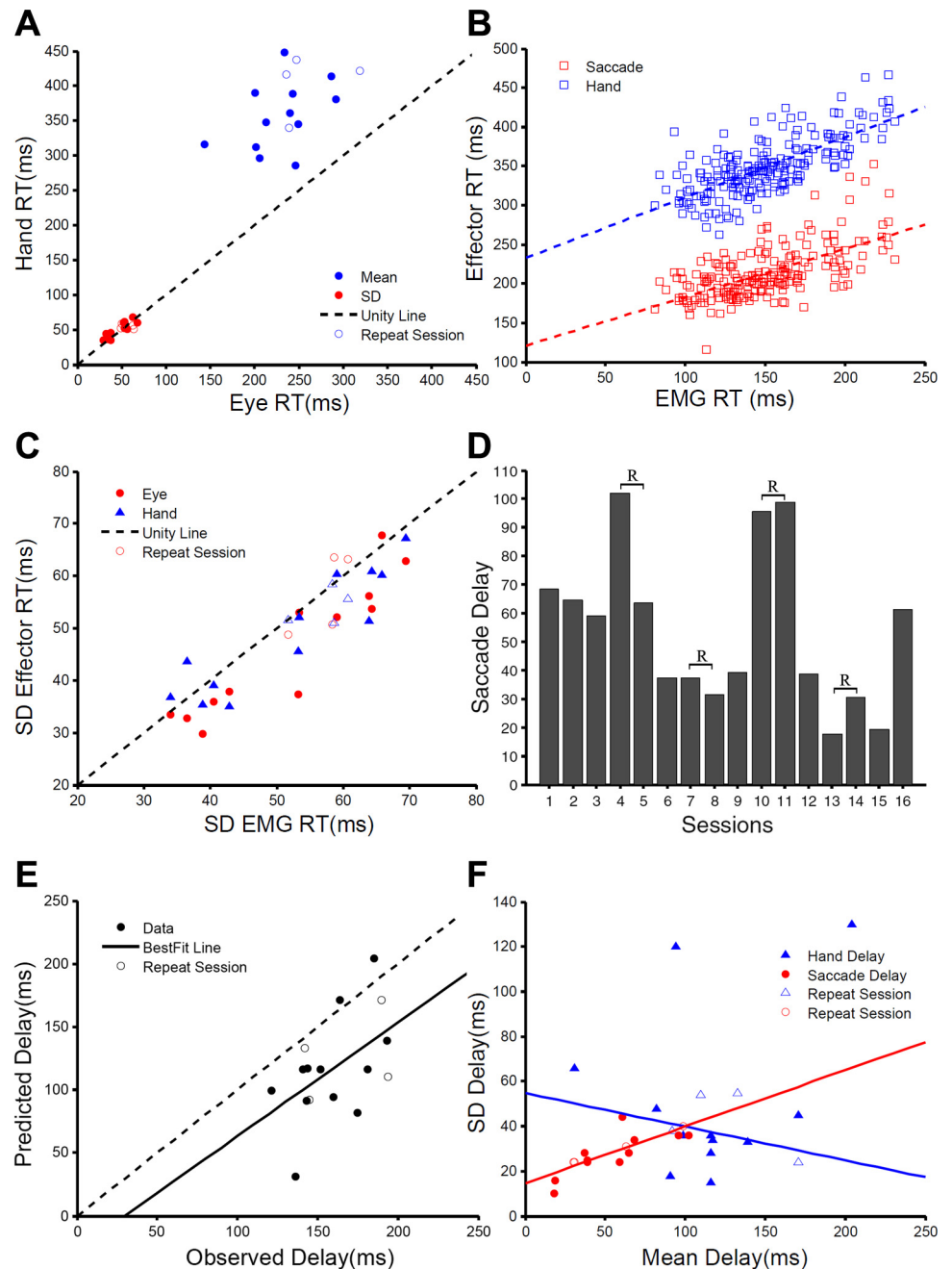


Fig. 5. Validation of the common command model. *A*: scatter plot of the means and SDs of eye and hand RT distributions. The SD of the hand RT does not scale with the mean. *B*: scatter plot of the trial-by-trial EMG onset latencies plotted against eye (red) and hand (blue) RTs for the same trial in a representative session. *C*: scatter plot of the SD of the EMG onset latencies plotted against SD of eye and hand RT for all the sessions. *D*: a bar plot of estimated saccade delay across all sessions. Subjects for whom sessions were repeated are marked with a “R”. *E*: scatter plot of the observed and predicted hand delay. The best fit line is represented by the solid black line. *F*: scatter plot of the means and the SDs of the estimated hand and saccade delays. The absence of correlation ($r = 0.22$, $P = 0.71$) indicates that the variance of the hand delay does not scale with the mean. The 4 extra recording sessions are denoted with open symbols throughout the panel.

Simulating the Common Command Model

Having estimated the parameters for the hand delay from the data, we tested whether a common command model with a delay and hand motor noise could explain the observed mean eye and hand RT distributions and their associated correlation for each subject. The model described in Fig. 7A assumes at least two common stages, a visual stage that selects a target and a movement planning stage that prepares the response (Thompson et al. 1996). The sensory input consisted of a single stochastic signal (generated from the RT distributions of the eye). Since the same sensory signal was fed into both eye and hand accumulators, a common movement plan accumulated to a common threshold. Once the threshold was reached, the eye movement was elicited, but the hand movement was elicited

after a mean delay that had a variable motor noise across trials. These free parameters were optimized from an individual subject's data and are tabulated in Table 1 (*experiment 1*) and Table 2 (*experiment 2*).

Figure 7B shows the comparison between the predicted and experimental cumulative RT distributions of both eye and hand effectors for a typical subject. The goodness of fit, accessed by calculating the r^2 , was on average 0.99, (max = 0.99, min = 0.98) for the eye RT distribution, and 0.99 (max = 0.99, min = 0.96) for the hand RT distribution. More importantly, a regression line plotted between the predicted and the experimental RT correlations revealed that this model [slope = 1, $r = 0.86$, $P < 0.001$, $n = 24$ sessions; data pooled across *experiments 1* ($n = 8$ subjects) and 2 ($n = 16$ sessions)] was a good predictor of the data across all but three of the sessions (Fig. 7C). These

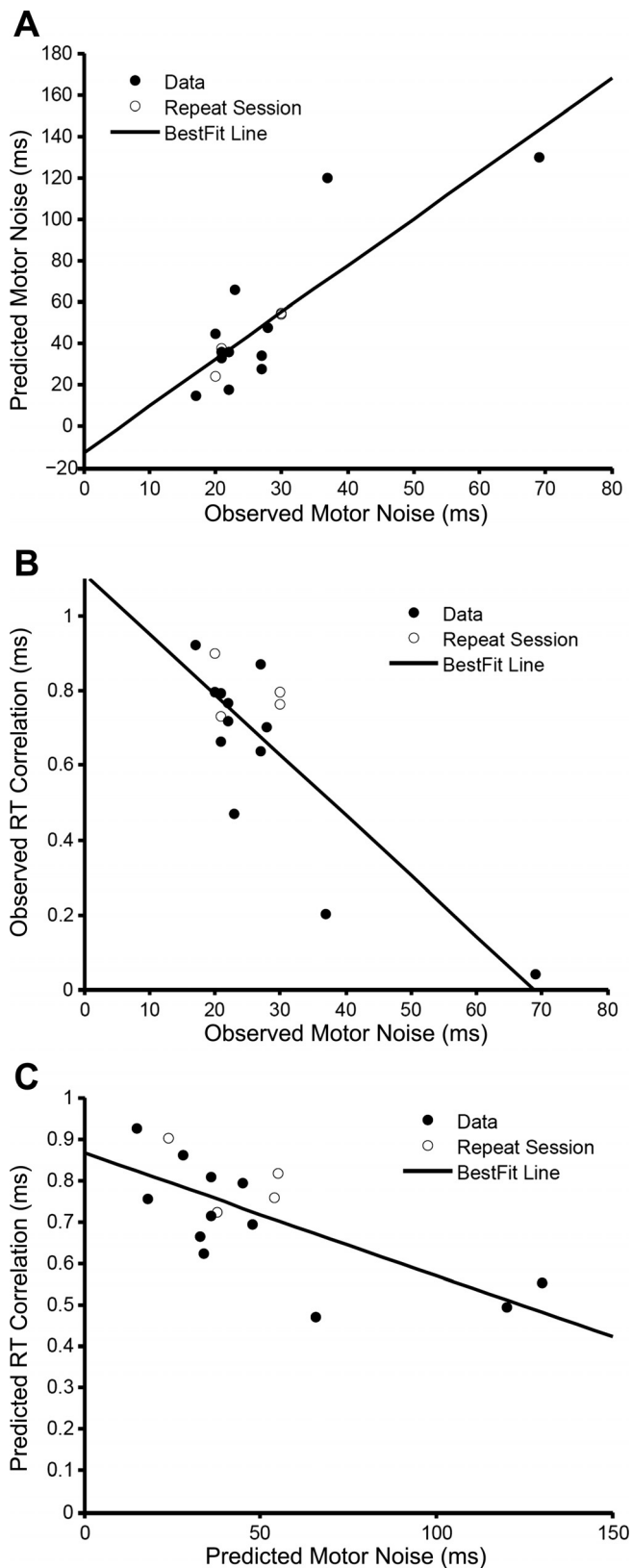


Fig. 6. Characterization of motor noise. A: scatter plot of the observed and predicted hand delay SD, operationally defined as motor noise. The best fit line is represented by the solid black line. B and C: scatter plot showing a negative linear relation between the eye-hand RT correlation and the predicted motor noise (C) estimated from the EMG (B). Best fit lines are also shown. The 4 extra recording sessions are denoted with open circles.

evidences strongly suggest that common command model is a physiologically valid model that can generate coordinated eye hand movements.

Simulating an Interacting Accumulator Model for Coordinated Eye-Hand Movements

Another architecture that could potentially explain the emergence of eye-hand coordination was recently proposed by Dean et al. (2011). They suggested that eye-hand RTs could be modeled as independent but interacting accumulators. We, therefore, tested the same model as an alternate possible architecture using the data obtained from *experiment 1*. The equations governing the accumulation for eye and hand were given by:

$$a_{GOe}(t) = a_{GOe}(t-1) + [\mu_{GOe} - \beta_{h>e} \cdot a_{GOh}(t-1)] + \xi_{GOe} \quad (2)$$

$$a_{GOh}(t) = a_{GOh}(t-1) + [\mu_{GOh} + \beta_{e>h} \cdot a_{GOe}(t-1)] + \xi_{GOh} \quad (3)$$

where, a_{GOe} and a_{GOh} represent the present level of GO unit activations for independent eye and hand accumulators at time t ; the mean drift rates for both accumulators are given by μ_{GOe} and μ_{GOh} , which represent the mean strength of the sensory signals; ξ_{GOe} and ξ_{GOh} are the Gaussian noise terms with zero mean and standard deviations of σ_{GOe} and σ_{GOh} , which represent the noise in the respective sensory signals. $\beta_{e>h}$ and $\beta_{h>e}$ are the coefficients that controls the strength of interaction between the eye and hand accumulators.

To estimate the parameters of the model, we initially fitted the eye and hand RT distributions in the independent condition individually based on a simple accumulator model and estimated the best fit parameters, which are tabulated in Table 3. These two accumulators thus accounted for the eye-alone and hand-alone conditions. These four parameters were subsequently used in the coupled interacting, accumulator model to generate the RT distributions of the eye (Fig. 8A) and hand (Fig. 8B) movements in the eye-hand condition. To estimate the parameters that govern the strength of interaction between eye and hand effectors, we used the observation that eye_{eh} RT distribution is slowed down by 44 ± 20 ms compared with the eye-alone condition ($\beta_{h>e}$), while the hand_{eh} RT distribution was speeded up by 80 ± 42 ms, relative to the hand-alone condition ($\beta_{e>h}$). The strength of interaction between the two accumulators, which were two additional free parameters of the interacting accumulator model (tabulated in Table 3), were thus optimized using the Monte Carlo methods to generate the eye and hand RT distributions in the coordinated condition. The goodness of fit between the experimental data and simulated RT distribution generated through the interactive model was 0.96 ± 0.04 and 0.99 ± 0.004 for the eye and hand RT distributions, respectively. The best fit line of the simulated and observed mean eye and hand RTs across subjects was close to the unity line (Fig. 8C) (slope_e = 0.89, slope_h = 0.95) and was also significantly correlated ($r_e = 0.94$, $P_e < 0.001$, $r_h = 0.97$, $P_h < 0.001$). This notwithstanding, the variances of the eye and hand RT distributions were significantly overestimated (Fig. 8D) by the model ($P_e = 0.04$, $P_h < 0.01$, Wilcoxon signed-rank test). We also tested if correlations between the eye and hand RTs emerged from the interactive accumulator

model (Fig. 9A), as shown earlier by Dean et al. (2011). However, due to the asymmetric nature of the interaction, which involves an inhibitory drive from the hand accumulator to eye accumulator, making it slower, and an excitatory drive

from the eye accumulator to the hand accumulator, making it faster, the predicted RT correlations were negative ($r = -0.22 \pm 0.04$), in contrast to the data (mean $r = 0.57 \pm 0.07$).

We also tested a variant of the interactive eye-hand accumulator model (Fig. 9B) in which inputs to the individual accumulators were correlated ($r = 1$). As done previously, the inputs to the accumulators, the strength of the sensory signal (μ_{GOe} and μ_{GOh}) and the extent of noise (σ_{GOe} and σ_{GOh}), were estimated from the RT distributions of the eye-alone and the hand-alone conditions. To implement this model, we generated two series of correlated random numbers, with 0 mean but variances controlled by σ_{GOe} and σ_{GOh} . These noise values were added to the mean strengths, μ_{GOe} and μ_{GOh} , at each time instant to generate stochastic, but correlated, sensory signals. These correlated stochastic signals were then accumulated to a threshold based on Eqs. 2 and 3. Although this model generated positive correlations between the eye and hand RTs; their magnitude was underestimated (mean $r = 0.26 \pm 0.07$) and not correlated with the data ($r = 0.13$, $P = 0.75$), as shown in Fig. 9C. Taken together, these simulations suggest that such a sequentially generated interactive accumulator model does not account for behavior in the coordinated eye-hand condition.

To quantify the relative superiority of the common command model over the interactive model, we used an Akaike Information Criterion (AIC) that penalizes a model with extra parameters, to select the model that best predicted the observed eye-hand RT correlations. The AIC value computed for the interactive accumulator model (92.70) and the interactive accumulator model with correlated inputs (80.96) was greater than the AIC value computed for the common command model (-14.87), suggesting that the common command model was the more parsimonious model that explained coordinated eye-hand behavior.

Common Command Model for the Independent Conditions

We tested if the same common command framework could account for the observed RTs in the eye-alone and hand-alone conditions, using the data from *experiment 1*. As alluded to in Fig. 2, *A* and *B*, the mean eye-alone RT across subjects was 44 ms faster than the mean eye in eye-hand or eye_{eh} RT, while the mean hand-alone RT across subjects was 80 ms slower than the mean hand in eye-hand or hand_{eh} RT. Unlike the eye-hand condition, in which the mean SDs of the eye and hand RT were comparable (mean eye SD = 79 ± 15 ms and mean hand SD = 87 ± 16 ms, $P = 0.3515$), the SDs of the RT for eye-alone and hand-alone were significantly different across subjects (mean

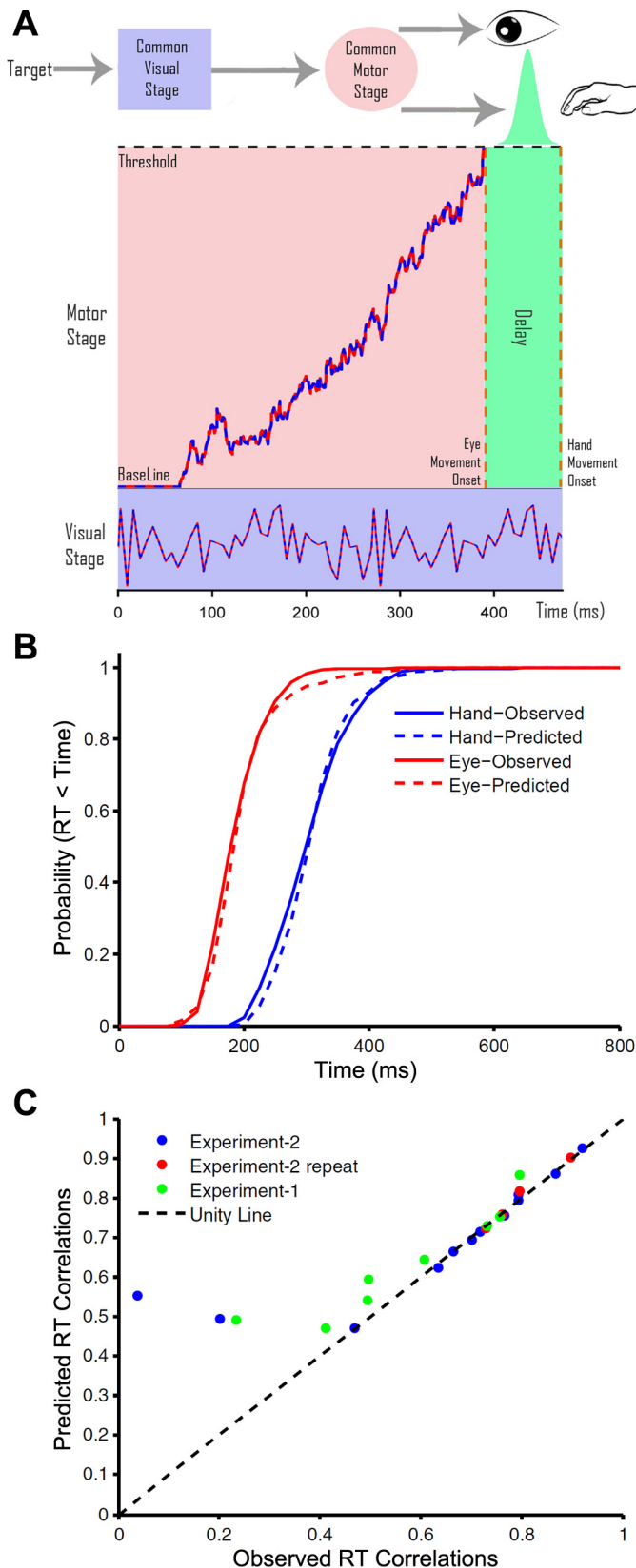


Fig. 7. Testing the common command model. *A*: schematic of the common command architecture. The purple square represents the visual stage where the target gets encoded, and the light pink circle represents the common movement preparation stage for the saccade and hand movement. The common stochastic sensory signal characterizing the visual stage is shown as a dashed red and blue trace. This signal is integrated over time in the common motor preparatory stage to reach a threshold indicated by the dashed black line. Saccades are immediately executed when the common signal reaches threshold, while the hand movement is executed after a temporal delay with Gaussian jitter (green). *B*: comparison between the observed (solid line) and predicted (dashed line) cumulative RT distributions for the saccade (red) and hand (blue). *C*: scatter plot of the observed vs. predicted eye-hand RT correlations across 24 sessions. The line of unity slope (black) is shown for reference. Data from *experiment 1* ($n = 8$, green) and *experiment 2* ($n = 12$, blue) and 4 repeat sessions in *experiment 2* ($n = 4$, red) are demarcated.

Table 1. Optimal parameters for the common command model in experiment 1

Redirect Trials	Common Command Eye Hand Condition						Common Command Alone Condition				
	Input Parameters				Goodness of Fit		Input Parameters			Goodness of Fit	
	μ	σ	Delay	Motor noise	R^2 Eye	R^2 Hand	μ	σ	Delay	R^2 Eye	R^2 Hand
Subject 1	0.0071	0.0286	113.6952	51.0355	0.9978	0.9976	0.006	0.0559	246.641	0.9973	0.9956
Subject 2	0.0039	0.0186	42.7401	90.935	0.9966	0.9856	0.0027	0.0652	259.3924	0.9941	0.9968
Subject 3	0.0037	0.0161	40.7011	40.9395	0.9949	0.9951	0.0052	0.0239	170.6264	0.9971	0.9531
Subject 4	0.0049	0.0285	37.7186	61.1	0.999	0.9944	0.0064	0.0264	86.0713	0.97	0.8664
Subject 5	0.0029	0.0243	147.5976	91.8	0.9876	0.9803	0.0035	0.0266	236.5124	0.9995	0.9916
Subject 6	0.004	0.017	55.4539	92.9335	0.9889	0.9951	0.0038	0.0211	92.6748	0.9863	0.9686
Subject 7	0.004	0.0232	102.1918	139.9335	0.9995	0.9721	0.0053	0.0308	113.9792	0.9978	0.935
Subject 8	0.0033	0.0227	128.0078	150.285	0.9985	0.9663	0.005	0.0275	259.426	0.9936	0.9746

Optimal parameters that fit the eye and hand reaction time (RT) distributions in the eye-hand condition with the common command model for the 8 subjects recorded on the redirect task are tabulated. Optimal parameters for the eye and hand RT when the alone condition was fitted with the common command model are also tabulated. μ , Strength of the sensory signals; σ , noise in the sensory signal.

eye SD = 82 ± 15 ms, mean hand SD hand = 123 ± 13 ms, $P < 0.001$). The significantly greater hand variability ($P < 0.001$) indicates that, unlike the eye-hand condition, variability scales with mean RT in the hand-alone condition. This relationship suggests that a common motor program rising to a single threshold cannot qualitatively explain RT distributions of the eye and hand when they are executed in isolation.

To quantitatively verify this intuition, we attempted to fit the hand-alone RT distribution to a common command model. We used the best fit parameters (Table 1) that could fit the eye-alone RT distribution to model the common command. The delay between the actual execution of the hand movement and the time at which the common command crossed the threshold was optimized and is tabulated in Table 1. Figure 10A shows the RT distribution for a typical subject, which indicates that, although the mean hand RT distribution was well estimated, its variance was underestimated. A similar trend was observed across the population (Fig. 10, B and C). The correlation between the predicted and observed means of the hand RT across subjects was 0.99 ($P < 0.001$). Since the best fit line had a slope of 0.99, no significant difference between the observed and the predicted mean hand RT was observed ($P = 0.58$, Wilcoxon signed-rank test). However, the variance estimated by the model and the data was not correlated ($r =$

-0.15 , $P = 0.73$), and the slope of the best fit line was -0.10 . Moreover, the predicted and observed variance of the hand RT distributions was significantly different ($P = 0.02$, Wilcoxon signed-rank test), suggesting that the common motor model underestimated the variance of the hand-alone RT distribution.

To further show that the common command model did not explain the RT distribution in the hand-alone condition, we assessed the EMG from the anterior deltoid muscles of the performing hand in four subjects who performed the hand-alone version of the pointing task (experiment 3). We compared the delay predicted by the common command model for the hand-alone condition with the observed delay calculated from the EMG data between the onset of EMG activity and the actual initiation of the hand movement. The mean observed delay (163 ± 30 ms, $n = 4$) was significantly lower than the mean predicted delay (217 ± 36 ms, $n = 8$, $P = 0.04$). Taken together, these data suggest that, while the common command model can explain $hand_{eh}$ RT distributions, the same model failed to account for the hand-alone RT distribution. This suggests that coordination may be achieved by a separate dedicated network that instantiates a common command architecture.

Table 2. Optimal parameters for the common command model in experiment 2

Eye-Hand EMG Trials	μ	σ	Delay	Motor Noise	R^2 Eye	R^2 Hand
Session 1	0.0043	0.0134	116.07	28	0.9979	0.9947
Session 2	0.0065	0.0152	138.68	33	0.9957	0.9962
Session 3	0.0069	0.0115	91.38	18	0.9962	0.9959
Session 4	0.0052	0.0130	30.58	66	0.9991	0.9809
Session 5	0.0054	0.0159	92.14	38	0.9952	0.997
Session 6	0.0053	0.0192	99.39	36	0.9966	0.9932
Session 7	0.0049	0.0126	115.58	15	0.9944	0.996
Session 8	0.005	0.0169	170.90	24	0.9977	0.9973
Session 9	0.0056	0.0113	116.82	34	0.9959	0.9978
Session 10	0.0043	0.0131	82.06	48	0.9955	0.9901
Session 11	0.0038	0.0147	109.67	54	0.9985	0.9932
Session 12	0.007	0.0215	116.25	36	0.9958	0.9944
Session 13	0.0038	0.0227	204.00	130	0.9556	0.9652
Session 14	0.0042	0.0211	133.01	55	0.9945	0.9872
Session-15	0.01	0.0583	170.89	45	0.9883	0.9617
Session 16	0.0045	0.0206	93.81	120	0.9886	0.9513

Optimal parameters that fit the eye and hand RT distributions in the eye-hand condition with the common command model for the set of 16 sessions are tabulated. The goodness of fit measured through R^2 is separately calculated and tabulated for the eye and hand distributions.

Table 3. *Optimal parameters for the interactive model in experiment 1*

Redirect Trials	Eye-Independent			Hand - Independent			Interactive Accumulators			
	μ	s	R^2	μ	s	R^2	$b_{h>e}$	$b_{e>h}$	R^2 Eye	R^2 Hand
Subject 1	0.006	0.0559	0.9973	0.0026	0.0121	0.9985	0.00067	0.0055	0.9644	0.9865
Subject 2	0.0027	0.0652	0.9941	0.0023	0.0119	0.0999	0.0078	0.0054	0.8777	0.9953
Subject 3	0.0052	0.0239	0.9971	0.0024	0.016	0.9977	0.0041	0.0023	0.9715	0.9887
Subject 4	0.0064	0.0264	0.97	0.0029	0.0267	0.9978	0.004	0.0033	0.9915	0.993
Subject 5	0.0035	0.0266	0.9995	0.0019	0.0116	0.9986	0.0022	0.00087	0.9724	0.9885
Subject 6	0.0038	0.0211	0.9863	0.0023	0.0194	0.9953	0.00001	0.00081	0.9856	0.9818
Subject 7	0.0053	0.0308	0.9978	0.0027	0.0187	0.9985	0.0039	0.00042	0.9735	0.9904
Subject 8	0.005	0.0275	0.9936	0.0021	0.0116	0.9995	0.0042	0.0011	0.9379	0.9967

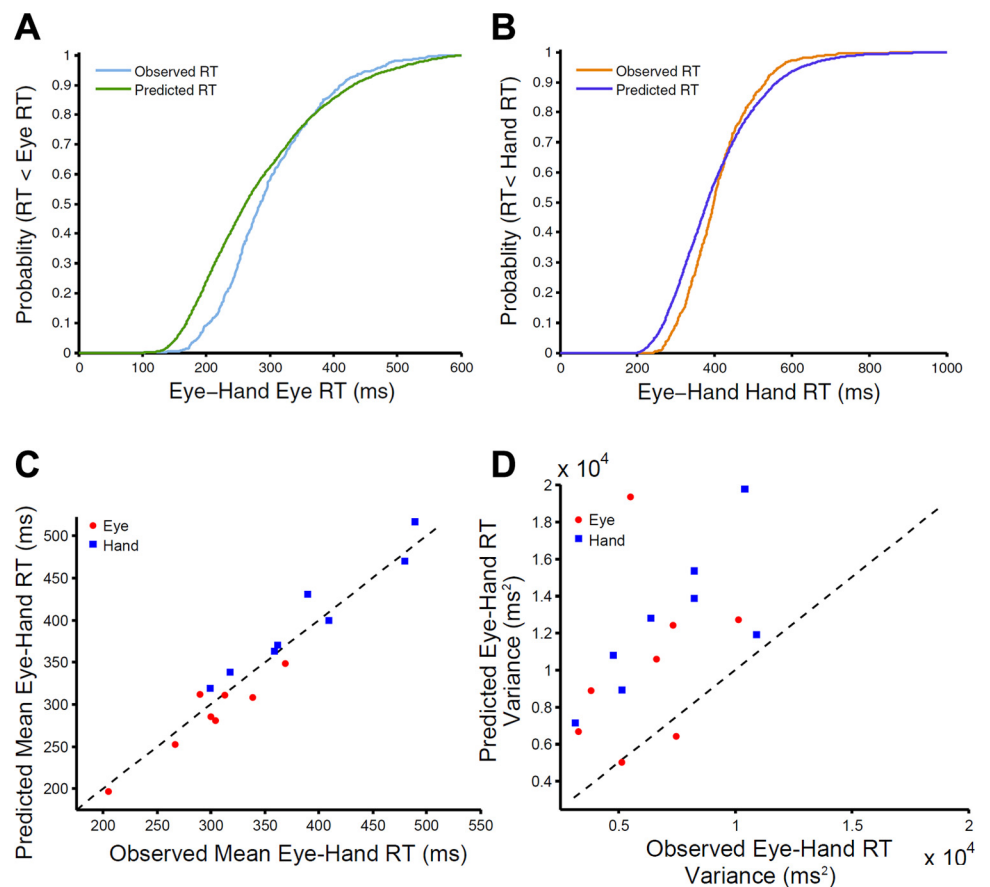
Optimal parameters obtained by fitting the eye-alone and hand-alone RT distributions based on the simple diffusion type accumulator model for the 8 subjects recorded on the redirect task are tabulated. The optimal interaction parameters and their goodness of fit obtained through the simulation of the interacting accumulator models that fit the eye and hand RT distributions in the eye-hand condition are also tabulated.

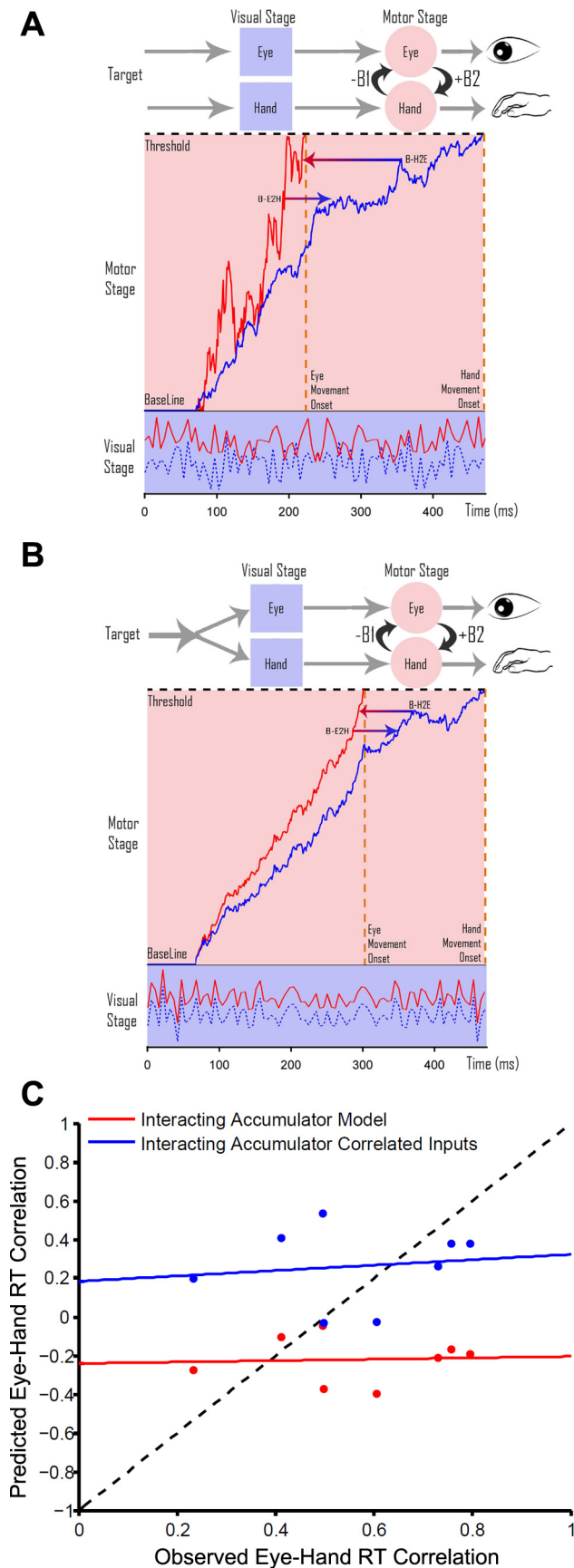
DISCUSSION

Other than the presence of strong RT correlations, changes in mean RTs in the eye-alone and hand-alone conditions relative to the eye-hand condition are potentially a signature for eye-hand coordination. Across subjects, we observed that saccade RTs were delayed, while hand RTs were shortened during eye-hand movements compared with their corresponding eye-alone and hand-alone conditions. Similar patterns have also been shown by others (Bekkering et al. 1994; Mather and Fisk 1985; Snyder et al. 2002). In contrast, other studies have reported shift in the means that are contradictory to what we have reported, i.e., on average, saccade RTs are faster and average hand RTs are delayed (Dean et al. 2011; Lunenburger et al. 2000) during eye-hand movements. One difference in our

task compared with others is that hand-alone, eye-alone and eye-hand conditions for the initial eight subjects were embedded in a task which required subjects to redirect their responses to a new target on infrequent random “step” trials. Although such a context is likely to have engaged proactive inhibitory mechanisms, which would delay responses in anticipation of step trials (Chiu et al. 2012; Farooqui et al. 2011), such delays are expected to be a common factor across all the conditions. In addition, we observed the same pattern of RT shifts between the hand-alone and eye-hand conditions for four subjects during which EMGs were recorded (*experiment 3*), even though these subjects did not have to redirect their responses. However, other nuances may have influenced the different results. For example, in the study with contrary results to ours (Dean et

Fig. 8. An interacting accumulator model does not explain the RT distribution in the eye-hand condition. *A* and *B*: cumulative distributions of observed and predicted saccades RT (cyan and green, respectively; *A*) and hand RT (orange and violet, respectively; *B*) distributions in the eye-hand condition for a representative subject. *C*: scatter plot of the observed and predicted mean saccade (red circles) and hand RT (blue squares) in the eye-hand condition. The data points close to the unity line (black dashed line) indicate a good fit to the model. *D*: scatter plot of the observed and predicted saccade (red circle) and hand (blue square) RT variance. Data above the unity line indicate that the model overestimated the variance, despite predicting the mean RT.

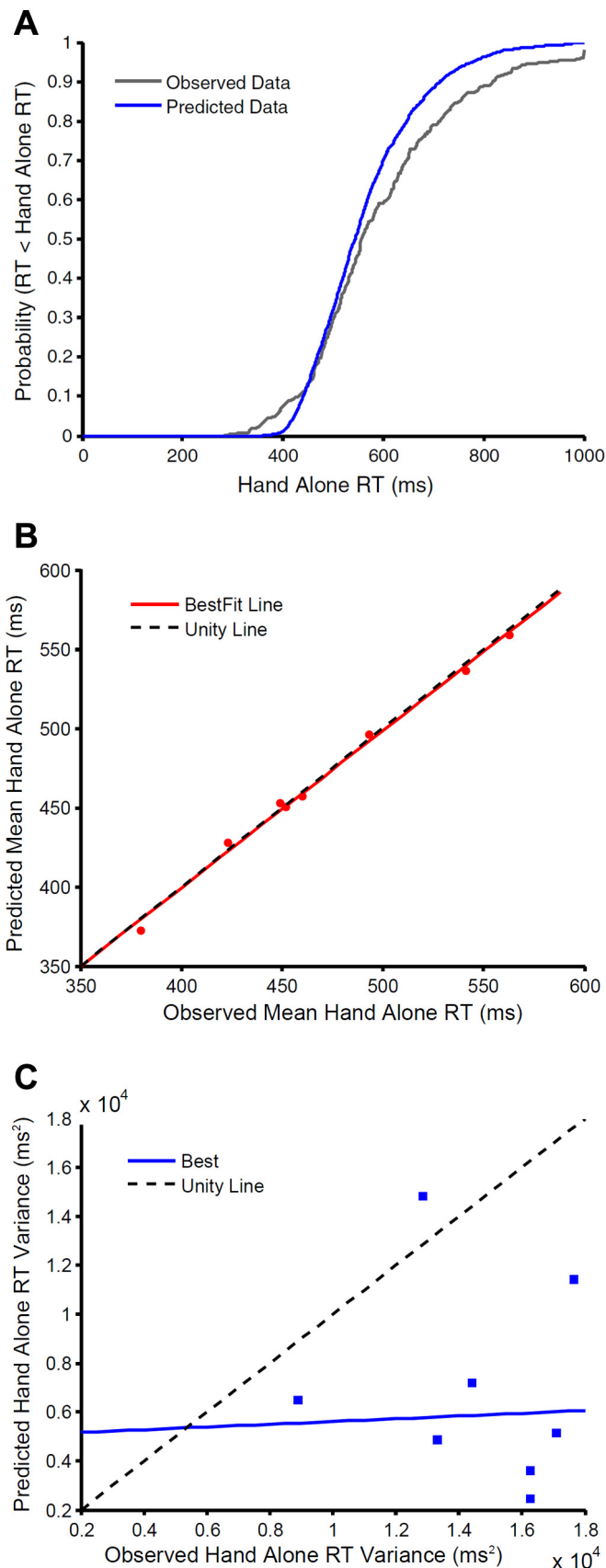




al. 2011), the data were collected from extremely well-trained nonhuman primates. Another source of difference across studies could be the nature of the block/session structure. For example, Dean et al. (2011) measured eye-alone, hand-alone, and eye-hand RTs in trials that were interleaved within a session, while we recorded subjects on eye-alone, hand-alone and eye-hand conditions on separate sessions. Although, in principle, pooling and comparing RTs across different sessions could be problematic, we counterbalanced the sessions across subjects. Furthermore, since every subject showed the same effect, we do not believe this to be a source of the difference. However, in interleaved trials, since subjects would have had to make an additional decision in each trial regarding the kind of response expected, this may have influenced the pattern of RTs across conditions. Despite these differences, in all studies of eye-hand coordination, saccade RTs were always faster than hand RTs, as we observed. However, the observation that the variance of the eye and hand were equal, despite differences in RT, indicate a common accumulator.

An attractive approach to model eye-hand coordination is to model eye and hand preparatory activity as independent but interacting accumulators (Dean et al. 2011). However, this model failed to explain the observed eye-hand data. Most importantly, while the model could explain the mean eye-hand RT, it overestimated the variance of the eye and hand RT distributions (Fig. 8D). Although the input to the hand accumulators had a larger variance, since it was modeled on the hand-alone RT, the excitatory drive from the eye moved the hand accumulation to threshold earlier. Since the resultant accumulation was shorter, the predicted variance was smaller than the original hand-alone RT variance from which it was derived. Yet this was not sufficiently small to explain the observed hand RT variance in the eye-hand condition; a stronger excitatory drive would be required to fit the variance with the observed data. The stronger excitatory drive, however, would lead to a faster mean hand RT than observed. Similarly, inhibitory drive from the hand accumulator onto the eye accumulator prolonged accumulation, resulting in the overestimation of the predicted eye RT variance in the eye-hand condition. Although lowering the strength of the inhibition could help fit the variance, this would underestimate the mean eye RT. This inability to fit the means and the variances of the

Fig. 9. An interacting accumulator model does not explain the RT correlations in the eye-hand condition. *A* and *B*: top panels represent a schematic of the interacting accumulator model. The purple squares represent the visual stages, and the light pink circles represent the movement preparation stages of the eye and hand movement, which are separate but coupled. Separate sensory signals are represented by the blue dashed line (hand) and the red solid line (eye). These stochastic signals for eye and hand are integrated separately and rise to threshold in the movement preparatory stage. The excitatory interaction from the eye to the hand accumulator is shown by the rightward arrow, and the inhibitory interaction between the hand to the eye accumulator is shown by a leftward arrow. *A*: a variant of the interacting accumulator model in which the inputs to the eye and hand accumulators are completely independent and de-correlated as shown by separate noisy stochastic sensory signals. *B*: a variant of the interactive accumulator model in which the inputs to the accumulators are completely correlated, as shown by separate noisy but correlated stochastic sensory signals. *C*: a scatter plot of the observed and predicted eye-hand RT correlations across subjects. Two variants of the interacting diffusion type accumulator were tested: an interacting model with uncorrelated inputs (red) and completely correlated inputs (blue). The best fit line (blue, red) is almost orthogonal to the unity line (dashed black). The interacting model fails to explain the observed data.



predicted eye and hand RT simultaneously highlights important limitations of previous eye-hand studies, in which model testing has been restricted to fitting means and correlations, while neglecting the role of RT variance as an important parametric constraint.

Differences between the Dean et al. (2011) study and ours are also likely to reflect task differences. In their study, a dual-task paradigm was employed, in which eye and hand movements were made to a target when cued. We suggest that having separate temporal delays for the initiation of eye and hand movements disrupted the natural coordination between the two effector systems. This is evident from the weaker RT correlation in their data compared with the present study. There were also differences in the modeling approaches used in that study. Although both approaches attempt to fit accumulators via drift diffusion, the approach taken was different. While we used the strength of μ and σ in the sensory signal to characterize the RT distributions, these two parameters were fixed to constant values in the Dean et al. (2011) study. Their fits were done by optimizing other parameters, like recruitment time constant (τ), residual time (T_o), strength of the recurrent excitation (α) and the strength of interaction between eye and hand accumulators (β_r and β_s). As a consequence, a direct comparison between parameters is not feasible. Another difference is that while Dean et al. only focused on the means of the eye and hand RT distributions and their dependence on stimulus onset asynchrony, we modeled a condition equivalent to the zero stimulus onset asynchrony condition in their study, but took into account the entire distribution, i.e., the means (Fig. 8C) as well as the variances (Fig. 8D), which enabled us to discount the interacting accumulator model. There were also differences in the approach to fitting the models. In the Dean et al. study, all the five parameters were optimized simultaneously. In contrast, we used a sequential method in which the RT distributions in the eye-alone and hand-alone conditions were used to constraint the inputs to the accumulators, while the RT distribution in the eye-hand condition helped to optimize the strength of the interactions. We believe this to be a more structured, data-driven method for estimating the strength of the interaction parameters. On the other hand, however, such a sequential approach may have reduced the overall degree of freedom, compromising the ability of the interactive model to fit the data. A more generous approach of freeing all six parameters simultaneously, when fitting eye and hand RT distribution in the coordinated eye-hand condition, although more likely to produce better fits, would certainly come at the cost of engendering multiple solutions. This notwithstanding, a consideration of Fig. 7C, suggests that, even if the eye-hand data were to be fitted by the interactive model, for 21 of the 24 sessions for which the common command model was almost a perfect fit (on the unity line), an AIC metric would certainly have penalized the 2 extra parameters in the interactive model. Taken together, our results suggest that the common command model outperforms the interactive model on the basis of par-

Fig. 10. The common command model does not explain the hand-alone and eye-alone conditions. *A*: observed (gray) and predicted (blue) hand-alone cumulative RT distributions. *B*: scatter plot of the observed and predicted hand-alone mean RT across subjects. *C*: scatter plot of the observed and predicted hand-alone RT variance. The data points below the unity line indicate underestimation of the observed variance by the model.

simony, as well as providing a deeper explanation for why the SDs of the eye and hand RT distributions are comparable, despite their mean RTs being significantly different.

Although the common command model accounted for the observed data, the model we implemented had a critical assumption in that the eye RT distribution was used as a proxy to model the common command. This assumption is not entirely valid, despite the relatively small inertia of the eye relative to the hand, and firing rates of frontal eye field neurons instantiating accumulation appear to reach the threshold 20–30 ms before the actual execution of the saccade. (Bruce and Goldberg 1985; Hanes and Schall 1996; Segraves and Park 1993). As a consequence, the common command model based on the eye RT distribution is expected to underestimate the observed temporal delay of the hand. Such an underestimation is what we observed (Fig. 5E) in our model prediction compared with the delays measured from the EMG. Nevertheless, despite this underestimation, a significant correlation between the predicted and observed delays (Fig. 5E), as well as strong correlations between the EMG and saccade onsets (Fig. 5B), suggests the applicability of the model. Another consequence of using the eye RT as a proxy of the common command is that the EMG and saccade onsets should coincide precisely with each other. However, we observed a discrepancy of 54 ms between the observed data and model prediction. We speculate that a large component of this delay may reflect the oculomotor efferent delay from the superior colliculus to saccade onset, which has been estimated to be about 30 ms from microstimulation studies (Robinson 1972; Schiller and Stryker 1972; Straschill and Rieger 1973).

The common command model also predicts a perfect correlation between saccade and hand RT, but it has been shown in our data, as well as in many other previous studies, that RT correlations covers a wide range (Biguer et al. 1982; Gielen et al. 1984; Herman et al. 1981; Mather and Fisk 1985). The common motor command with effector-specific noise can account for such heterogeneity. The model also predicted a negative correlation between the RT correlation of eye and hand with the motor noise. Interestingly, we were able to show a similar trend between the RT correlation and motor noise measured from EMG (Fig. 6B). This is another physiological validation of the common command model. It also suggests that the peripheral motor noise can be a major component in de-correlating the perfect RT correlation predicted by the common command model between the eye and hand.

Although, the present data suggest a common command architecture underlying eye-hand coordination, it is possible that under more challenging behavioral contexts a more flexible means of coordination maybe recruited. Under such contexts, an interactive accumulator model might provide a better model to understand eye-hand coordination. Here we have shown that the common command architecture is also used to generate coordinated movements under relatively simple conditions, like pointing, that generate strong eye-hand correlations, in contrast to the more complicated dual-task condition employed by Dean et al. (2011), in which the correlations were much lower. Interestingly, in our own dataset, the behavior in 3 sessions out of 24 which could not be accounted for by the common command model were all characterized by similar low eye-hand RT correlations. Thus, in these three sessions,

subjects might have recruited a different strategy to accomplish the task.

ACKNOWLEDGMENTS

We thank Sheldon Hoffmann (Reflective Computing) for software support, and Puneet Singh for the preparing the 3D schematic of the experimental setup.

GRANTS

This work was supported by grants from the Department of Science and Technology (IRHPA), Government of India, and core funding from the National Brain Research Centre. A. Gopal was supported by a fellowship from the National Brain Research Centre.

DISCLOSURES

No conflicts of interest, financial or otherwise, are declared by the author(s).

AUTHOR CONTRIBUTIONS

Author contributions: A.G. and A.M. conception and design of research; A.G. and P.V. performed experiments; A.G. analyzed data; A.G. and A.M. interpreted results of experiments; A.G. prepared figures; A.G. drafted manuscript; A.G. and A.M. edited and revised manuscript; A.G., P.V., and A.M. approved final version of manuscript.

REFERENCES

- Bekkering H, Adam JJ, Huson A, Kingma H, Whiting HTA.** Reaction time latencies of eye and hand movements in single- and dual-task conditions. *Exp Brain Res* 97: 471–476, 1994.
- Biguer B, Jeannerod M, Prablanc C.** The coordination of eye, head, and arm movements during reaching at a single visual target. *Exp Brain Res* 46: 301–304, 1982.
- Bizzi E, Kalil RE, Tagliasco V.** Eye-head coordination in monkeys: evidence for centrally patterned organization. *Science* 173: 452–454, 1971.
- Bock O.** Coordination of arm and eye movements in tracking of sinusoidally moving targets. *Behav Brain Res* 24: 93–100, 1987.
- Bruce CJ, Goldberg ME.** Primate frontal eye fields. I. Single neurons discharging before saccades. *J Neurophysiol* 53: 603–635, 1985.
- Carpenter RH, Williams ML.** Neural computation of log likelihood in control of saccadic eye movements. *Nature* 377: 59–62, 1995.
- Chiu YC, Aron AR, Verbruggen F.** Response suppression by automatic retrieval of stimulus-stop association: evidence from transcranial magnetic stimulation. *J Cogn Neurosci* 24: 1908–1918, 2012.
- Dean HL, Marti D, Tsui E, Rinzel J, Pesaran B.** Reaction time correlations during eye-hand coordination: behavior and modeling. *J Neurosci* 31: 2399–2412, 2011.
- Farooqui AA, Bhutani N, Kulashekhar S, Behari M, Goel V, Murthy A.** Impaired conflict monitoring in Parkinson's disease patients during an oculomotor redirect task. *Exp Brain Res* 208: 1–10, 2011.
- Fisk JD, Goodale MA.** The organization of eye and limb movements during unrestricted reaching to targets in contralateral and ipsilateral visual space. *Exp Brain Res* 60: 159–178, 1985.
- Gielen CC, van den Heuvel PJ, van Gisbergen JA.** Coordination of fast eye and arm movements in a tracking task. *Exp Brain Res* 56: 154–161, 1984.
- Gribble PL, Everling S, Ford K, Mattar A.** Hand-eye coordination for rapid pointing movements. Arm movement direction and distance are specified prior to saccade onset. *Exp Brain Res* 145: 372–382, 2002.
- Hanes DP, Schall JD.** Neural control of voluntary movement initiation. *Science* 247: 427–430, 1996.
- Herman R, Herman R, Maulucci R.** Visually triggered eye-arm movements in man. *Exp Brain Res* 42: 392–398, 1981.
- Karst GM, Hasan Z.** Timing and magnitude of electromyographic activity for two-joint arm movements in different directions. *J Neurophysiol* 66: 1594–1604, 1991.
- Luce RD.** *Response Times: Their Role in Inferring Elementary Mental Organization.* Oxford, UK: Oxford UP, 1986.
- Lunenburg L, Kutz DF, Hoffmann KP.** Influence of arm movements on saccades in humans. *Eur J Neurosci* 12: 4107–4116, 2000.

- Mather JA, Fisk JD.** Orienting to targets by looking and pointing: Parallels and interactions in ocular and manual performance. *Q J Exp Psychol A* 37: 315–338, 1985.
- Ramakrishnan A, Chokhandre S, Murthy A.** Voluntary control of multi-saccade gaze shifts during movement preparation and execution. *J Neurophysiol* 103: 2400–2416, 2010.
- Ratcliff R.** A theory of memory retrieval. *Psychol Rev* 85: 59–108, 1978.
- Ratcliff R, Van Dongen HP.** Diffusion model for one-choice reaction-time tasks and the cognitive effects of sleep deprivation. *Proc Natl Acad Sci U S A* 108: 11285–11290, 2011.
- Ray S, Schall JD, Murthy A.** Programming of double-step saccade sequences: modulation by cognitive control. *Vision Res* 44: 2707–2718, 2004.
- Reddi BA, Asrress KN, Carpenter RH.** Accuracy, information, and response time in a saccadic decision task. *J Neurophysiol* 90: 3538–3546, 2003.
- Reddi BA, Carpenter RH.** The influence of urgency on decision time. *Nat Neurosci* 3: 827–830, 2000.
- Robinson DA.** Eye movements evoked by collicular stimulation in the alert monkey. *Vision Res* 12: 1795–1808, 1972.
- Rogal L, Reible G, Fischer B.** Reaction times of the eye and the hand of the monkey in a visual reach task. *Neurosci Lett* 58: 127–132, 1985.
- Sailer U, Eggert T, Ditterich J, Straube A.** Spatial and temporal aspects of eye-hand coordination across different tasks. *Exp Brain Res* 134: 163–173, 2000.
- Schall JD, Hanes DP.** Neural mechanisms of selection and control of visually guided eye movements. *Neural Netw* 11: 1241–1251, 1998.
- Schiller PH, Stryker M.** Single-unit recording and stimulation in superior colliculus of the alert rhesus monkey. *J Neurophysiol* 35: 915–924, 1972.
- Segraves MA, Park K.** The relationship of monkey frontal eye field activity to saccade dynamics. *J Neurophysiol* 69: 1880–1889, 1993.
- Snyder LH, Calton JL, Dickinson AR, Lawrence BM.** Eye-hand coordination: saccades are faster when accompanied by a coordinated arm movement. *J Neurophysiol* 87: 2279–2286, 2002.
- Straschill M, Rieger P.** Eye movements evoked by focal stimulation of the cat's superior colliculus. *Brain Res* 59: 211–227, 1973.
- Thompson KG, Hanes DP, Bichot NP, Schall JD.** Perceptual and motor processing stages identified in the activity of macaque frontal eye field neurons during visual search. *J Neurophysiol* 76: 4040–4055, 1996.
- Usher M, McClelland JL.** The time course of perceptual choice: the leaky, competing accumulator model. *Psychol Rev* 108: 550–592, 2001.
- Wagenmakers EJ, Brown S.** On the linear relation between the mean and the standard deviation of a response time distribution. *Psychol Rev* 114: 830–841, 2007.
- Wagenmakers EJ, Grasman RP, Molenaar PC.** On the relation between the mean and the variance of a diffusion model response time distribution. *J Math Psychol* 49: 195–204, 2005.

